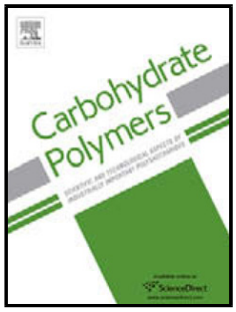

Title: Grafting of polyethylenimine onto cellulose nanofibers for interfacial enhancement in their epoxy nanocomposites

Author: Jiangqi Zhao Qingye Li Xiaofang Zhang Meijie Xiao Wei Zhang Canhui Lu

PII: S0144-8617(16)31290-5
DOI: http://dx.doi.org/doi:10.1016/j.carbpol.2016.11.025
Reference: CARP 11737

To appear in:

Received date: 10-9-2016
Revised date: 4-11-2016
Accepted date: 8-11-2016

Please cite this article as: Zhao, Jiangqi., Li, Qingye., Zhang, Xiaofang., Xiao, Meijie., Zhang, Wei., & Lu, Canhui., Grafting of polyethylenimine onto cellulose nanofibers for interfacial enhancement in their epoxy nanocomposites.*Carbohydrate Polymers* http://dx.doi.org/10.1016/j.carbpol.2016.11.025

Grafting of Polyethylenimine onto Cellulose Nanofibers for Interfacial Enhancement in Their Epoxy Nanocomposites

Jiangqi Zhao, Qingye Li, Xiaofang Zhang, Meijie Xiao, Wei Zhang* and Canhui Lu*

State Key Laboratory of Polymer Materials Engineering, Polymer Research Institute at Sichuan University, Chengdu 610065, China

**Authors for correspondence. E-mail: weizhang@scu.edu.cn (W. Zhang), canhuilu@263.net (C. Lu); Phone: 86-28-85460607; Fax: 86-28-85402465.*

Highlights

- ► CNFs-PEI was synthesized as both a reinforcing filler and a curing agent for epoxy.
- ► CNFs-PEI increased the crosslinking density and strengthened the interface.
- ► The mechanical properties of the nanocomposites were greatly improved.
- ► Incorporation of CNFs-PEI remarkably reduced the CTE of the epoxy nanocomposites.
- ► The thermal conductivity of the nanocomposites was observed to increase.

Abstract

Cellulose nanofibers (CNFs) were surface-modified with polyethyleneimine (PEI), which brought plentiful amine groups on the surface of CNFs, leading to a reduced hydrogen bond density between CNFs and consequently less CNFs agglomerates. The amine groups could also react with the epoxy as an effective curing agent that could increase the interfacial crosslinking density and strengthen interfacial adhesion. The tensile strength and Young's modulus of CNFs-PEI/Epoxy nanocomposites were 88.1% and 237.6% higher than those of neat epoxy, respectively. The tensile storage modulus of the nanocomposites also increased significantly at the temperature either below or above the Tg. The coefficient of thermal expansion for the CNFs-PEI/Epoxy nanocomposites was 22.2 $ppm \cdot K^{-1}$, much lower than that of the neat epoxy (88.6 $ppm \cdot K^{-1}$). In addition, the thermal conductivity of the nanocomposites was observed to increase as well. The exceptional and balanced properties may provide the nanocomposites promising applications in automotive, construction and electronic devices.

Keywords: cellulose nanofibers (CNFs), coefficients of thermal expansion (CTE), epoxy resin, polyethylenimine (PEI), nanocomposites, interfacial enhancement.

1. Introduction

Fiber reinforced polymer composites have been used widely as primary load-bearing structures in the lightweight construction, such as automotive and aerospace industry, due to their combination of excellent mechanical properties along with the low density (Akil et al., 2011; Jia et al., 2013). In recent years, growing environmental awareness around the world has enhanced the interest in the use of natural fibers as an alternative to traditional synthetic fibers in composite materials (Masoodi, El-Hajjar, Pillai, & Sabo, 2012). Cellulose, the world's most abundant natural polymer, is becoming more and more important as a renewable resource to replace petroleum-based materials, because of its renewable and biodegradable nature

(Klemm, 2011). In addition to the above-mentioned advantages of cellulose, nanocellulose, particularly cellulose nanofibers (CNFs), exhibits many other unique characteristics, including high aspect ratio, high strength and stiffness, ease for chemical modification, and the ability to form highly porous mesh (Moon, Martini, Nairn, Simonsen, & Youngblood, 2011; Yang, Shi, Zhitomirsky, & Cranston, 2015). CNFs are considered to be the ideal material on which to base a new biopolymer composites industry, and an extensive list of nanocomposites comprising CNFs has been explored (Inui, Koga, Nogi, Komoda, & Suganuma, 2015; Ansari, Skrifvars, & Berglund, 2015).

Epoxy resins are an important class of thermosetting polymers with extensive applications in coatings, adhesives, electronics and others (Omrani, Simon, & Rostami, 2008). To date, there have been a few reports on the reinforcement of epoxy composites using cellulose fibers (Omrani, Simon, & Rostami, 2008; Low et al., 2007). However, compared with other commonly used fillers like glass fibers, cellulose fibers usually exhibit inferior enhancement of the composites' mechanical properties. The mechanical behavior of composites depends strongly on the dispersion of the fillers in matrix as well as the interfacial interaction between them (Liu, Pourrahimi, Olsson, Hedenqvist, & Gedde, 2015). However, the numerous hydroxyl groups on the cellulose molecules give rise to strong polarity of cellulose and dense hydrogen bonds in its structure (Nishiyama, Sugiyama, Chanzy, & Langan, 2003). As a consequence, the compatibility and dispersion of CNFs were not satisfied in many polymeric matrices, especially at high loading conditions (Lu et al., 2013; Lu et al., 2014). These defects reduce the mechanical properties of the composites and severely limit the applications of cellulose in composite materials. Thus the poor dispersion and compatibility between cellulose fibers and polymer matrix become the key issues that must be overcome in order to produce high-performance composites. It should also be noted that most early studies were focused mainly on the mechanical properties of cellulose/epoxy composites and ignored some other important features (e.g., thermal conductivity and coefficient of thermal expansion (CTE)) (Sakakibara, Yano, & Tsujii, 2016; Suzuki et al., 2014; Omrani, Simon, & Rostami, 2008).

Considering the intensive applications of epoxy in the heat-generating parts of electronic devices such as integrated circuits, it is desired to increase the thermal conductivity and lower the CTE of epoxy. Otherwise, severe deformation or even damage of the devices might be occurred.

Various methods have been developed to modify the surface properties of cellulose, such as alkali treatment (Lu et al., 2013), acetylation (Ashori, Babaee, Jonoobi, & Hamzeh, 2014), oxidation (Miao, & Hamad, 2013), coupling agent treatment (Kargarzadeh, Sheltami, Ahmad, Abdullah, & Dufresne, 2015), and so on. However, the mechanical properties of the resulting composites were still far from satisfaction. For example, Lu et al. found that after the NaOH pretreatment of cellulose fibers, the maximum tensile strength of the cellulose/epoxy composites was increased only by 34% (Lu et al., 2013). For the coupling agent treatment, Lu et al. reported the storage modulus of the cellulose/epoxy composite was increased from 2.6 GPa to 3.1 GPa after the modification (Lu, Askeland, & Drzal, 2008). It is noteworthy that chemical modification may detrimentally change the structure of cellulose fibers to some extent and consequently sacrifice their mechanical properties (Missoum, Belgacem, & Bras, 2013).

Polyethylenimine (PEI) is a branched polymer with plentiful amine groups on its molecular chains (Liu, & Huang, 2011). Compared with most of the commercial coupling agents, the amine density of PEI is much higher (Zhou, 2011; Xie, Hill, Xiao, Militz, & Mai, 2010). Since the amine groups are capable to react with epoxy groups, the grafted PEI could covalently bridge the fillers and the epoxy matrix. Actually, early studies have already demonstrated that PEI is a good candidate to functionalize fillers and improve the interfacial properties in the composites (Tang et al., 2015; Ma et al., 2015). However, most of these studies were based on the PEI-modified carbon materials. Besides, there is also no comprehensive understanding of the curing reactions between PEI and epoxy so far.

In this study, CNFs were mechanically extracted from filter paper and subsequently surface-modified with PEI. The grafted PEI on the CNFs was expected to generate covalent bonds between CNFs and epoxy (see Figure 1 for the schematic of the

preparation process as well as the reaction mechanism). Meanwhile, the 3D CNFs network skeleton in the epoxy matrix could act as efficient pathways for stress and phonons transfer, thus providing the nanocomposites with excellent mechanical properties as well as a high thermal conductivity and a low CTE.

2. Experimental

2.1. Materials

Cellulose filter paper was supplied by Fushun Civil Affairs filter paper factory. A branched polyethylenimine (PEI, average M_w of 25000) was purchased from Sigma Aldrich. Bisphenol A epoxy resin was provided by Xingchen Synthetic Material Co., Ltd. (Nantong, China), and the epoxy value was 0.44. The curing agent of 4,4-diamino diphenyl methane (DDM) was provided in the analytical grade by Sinopharm Chemical Reagent Co., Ltd. (Shanghai, China). Methyl methacrylate (MMA), ethylenediamine (EDA) and other chemicals were of analytical grade and purchased from Chengdu Kelong Chemicals Co., Ltd. (Sichuan, China).

2.2. Preparation of CNFs

The filter paper was cut into small pieces and soaked in distilled water for 12 h. Then, the paper fibers were dispersed in distilled water using an emulsifying machine (MXR-1450, Muxuan, China) at a rotation speed of 3000 rpm for 10 min. The obtained suspension (0.5 wt.%) was treated by a horn-type ultrasonic generator (JY99-IIDN, Scientz, China) at an output power of 1200 W for 30 min. Finally, a high shear homogenizer (T18, IKA, Germany) was used to isolate CNFs at a rotation speed of 20000 rpm for 1 h.

2.3. Preparation of CNFs-PEI porous films

A schematic depiction of the grafting process was presented in Figure S1. Firstly, EDA was introduced onto the surface of CNFs. 1.0 g of CNFs was dispersed in 100 mL of distilled water under the nitrogen atmosphere, and 1.5 g of MMA was slowly added with cerium ammonium nitrate (6 mmol dm^{-3}) as an initiator. The reaction was

conducted at the room temperature for 3 h under magnetic stirring. The products were washed three times with methanol and subsequently reacted with 1.5 g of EDA in a methanol solution, which was lasted for 24 h at 60 ºC. The as-prepared EDA-modified CNFs were marked as CNFs-EDA, which was further reacted with PEI. 1.0 g of CNFs-EDA was immersed in 50 mL of PEI solution in methanol (2 wt.% PEI) for 24 h under magnetic stirring at room temperature. Then, 200 mL of 1 wt.% glutaraldehyde solution was added, and the system was further stirred for 30 minutes. The final products were washed thoroughly with distilled water, and marked as CNFs-PEI.

The wet films of CNFs-PEI were prepared by ultrafiltration of the fiber slurries using a 0.22 μm microporous membrane (Xinya Purification Device Co., Ltd., Shanghai, China). The wet films were rapidly frozen in liquid nitrogen (-196 ºC) and placed in a freeze-drying chamber (FD-1A-50, Biocool, China). The freeze-drying process was maintained at -30 ºC for 24 h to obtain the CNFs-PEI porous films. For comparison, the CNFs films were prepared in the same way.

2.4. Preparation of CNFs-PEI/Epoxy nanocomposites

The epoxy resin was diluted with acetone (20 wt.%) to improve its mobility and permeability. A certain amount of DDM was added to the diluted epoxy and stirred to form a uniform mixture. The as-prepared CNFs-PEI porous films with dimensions of 10 × 50 mm were soaked in the mixture of epoxy/acetone/DDM until they became entirely impregnated by the solution. The solvent in the mixture was evaporated in a vacuum oven at 60 ºC for 2 h. Finally, the impregnated films were sandwiched by glass slides and cured at 80 ºC for 2 h and then 140 ºC for 2 h to obtain the CNFs-PEI/Epoxy nanocomposites. For comparison, CNFs/Epoxy nanocomposites and neat epoxy were prepared using the same procedure. The content of CNFs or CNFs-PEI in the nanocomposites was about 30%.

2.5. Material characterizations.

The morphologies of original cellulose fibers (OCFs) and CNFs before and after modification were observed using a scanning electron microscopy (SEM, Inspect F 50, FEI, USA). The liquid-nitrogen-fractured surface of the nanocomposite films was also examined by SEM. The chemical structure of samples was characterized by FTIR and XPS, respectively. FTIR analysis was performed from 4000 to 500 cm^{-1} at a resolution of 2 cm^{-1} using a Nicolet 560 FTIR spectrometer. XPS spectra were recorded on a Kratos XASAM 800 spectrometer with an Al Ka X-ray source (1486.6 eV).

The curing behaviors of the CNFs-PEI/Epoxy nanocomposites without DDM were evaluated by differential scanning calorimetry (DSC) and gel content measurement. The DSC data were examined with a Netzsch 204F1 DSC apparatus in a temperature range from 25 to 250 ^{o}C at heating rates of 5, 10, 15, and 20 ^{o}C/min, respectively. The epoxy resin and CNFs-PEI were mixed homogeneously at 1:1 ratio, and the mixture was subsequently refrigerated (-15℃) for 24 h before the measurement. For comparison, the curing behaviors of neat epoxy with DDM were analyzed at the same conditions, while the pure epoxy without any curing agent was also analyzed at a heating rate of 10 ^{o}C/min. For the gel content measurement, the epoxy resin was mixed with different proportions of CNFs-PEI, and the mixtures reacted at 80 ^{o}C for 2 h and then 140 ^{o}C for 2 h. After reaction, the composites were extracted with acetone using a Soxhlet apparatus until no more epoxy could be extracted, and the resulting residues were dried in vacuum at 100 ^{o}C to a constant weight. The gel fraction was determined by the following equation:

$$Gel\,\% = (W_2 - W_0)/(W_1 - W_0) \times 100\% \quad (1)$$

where W_0 was the weight (g) of CNFs-PEI; W_1 and W_2 were the weights (g) of composites before and after extraction, respectively.

The mechanical properties of the nanocomposites were measured using a universal testing machine (Instron 5567, USA) at a crosshead speed of 1 mm/min. Ten specimens were tested for each sample and the average value was reported. Dynamic mechanical analysis (DMA) was conducted on a DMA 2980 (TA, USA), and the specimens were prepared in dimensions of approximately 25 × 5 mm. Temperature

scans were run from the room temperature to 250 ^{o}C at a heating rate of 3 ^{o}C/min and a frequency of 1 Hz. The coefficient of thermal expansion (CTE) of the nanocomposites was characterized by a thermomechanical analyzer (TMA 2940, TA, USA) from the room temperature to 200 ^{o}C at a heating rate of 5 ^{o}C/min. The thermal conductivity of the nanocomposites (5 mm in height and 25 mm in diameter) was measured by a Hot Disk thermal conductivity detector (model 1500, Sweden).

3. Results and discussion

3.1. Characterization of the cellulose fibers.

Figure 1a and b display the optical images of the 0.1 wt.% dispersions of OCFs and CNFs after being left to stand for 3 days. Clear sedimentation was observed in the OCFs dispersion, whereas the CNFs could be homogeneously dispersed in distilled water without noticeable sedimentation, indicative of the substantial changes in the fiber diameter. As shown in Figure 2a, the OCFs exhibited a banded morphology with diameters in the range of 20-50 μm. After the physical nanofibrillation process, the cellulose fibers were almost completely disintegrated into CNFs with diameters in the range of 20-70 nm (Figure 2b). Meanwhile, the surface chemical modification provided the CNFs with a much rougher surface (Figure 2c) and obviously thicker fiber diameters (50-150 nm) as compared with the precursor CNFs, which was consistent with the grafting of PEI. The CNFs-PEI could also be evenly dispersed in distilled water, and the dispersion was orange-yellow in color (Figure 1c).

The cross-sectional features of the freeze-dried films are shown in Figure S2. Both films, either with or without PEI grafting, display a highly porous structure. The massive open pores would allow the penetration of the epoxy solution and accommodate the resin in the composite films. Clear sheet-like structure was observed on the cross-section of the CNFs films. This resulted from the compressive forces during the growth of ice crystals coupled with hydrogen bond formation among fibers, leading to the agglomeration of CNFs (Zhang, Zhang, Lu, & Deng, 2012). By contrast, only a few sheet-like agglomerates were found in the CNFs-PEI film, possibly due to the surface modification that can reduce the hydrogen bonding density among CNFs.

As a consequence, a more uniform dispersion of CNFs-PEI in the epoxy matrix could be achieved.

FTIR spectra (Figure 2d) were collected to elucidate the chemical structure changes of CNFs after the surface modification. Compared with the spectrum of unmodified CNFs, an absorption peak at 1740 cm^{-1} appeared in CNFs-EDA and CNFs-PEI owing to the presence of ester groups. It suggested that MMA had been grafted to CNFs, and the reaction between esters and ethylenediamine was incomplete for this solid-liquid reaction (Zhang, Wang, Xu, & Cheng, 2012). The absorption peaks at 1640, 1560 and 1450 cm^{-1} were assigned to amide and amine groups (Song, & Xu, 2013;), and the absorption peaks at 2850, and 2930 cm^{-1} were assigned to methylene groups (Song, & Xu, 2013). Compared with that of CNFs-EDA, the relative intensities of these peaks significantly increased in the CNFs-PEI spectrum, which manifested that PEI had been grafted onto CNFs.

XPS was used to characterize the surface elements and chemical composition in a quantitative manner. The XPS spectra of these samples were shown in Figure 2e and S3. No nitrogen signal was detected for the CNFs sample (Figure S3a). In contrast, a strong nitrogen peak appeared at around 399.3 eV for the CNFs-EDA (Figure S3b) and CNFs-PEI (Figure 2e). These results further confirmed the successful grafting of PEI to the CNFs' surface (Zhao et al., 2015). The nitrogen content of CNFs-PEI was estimated to be 15.85%, significantly higher than that of CNFs-EDA (see Table S1), suggesting that numerous amine groups had been tethered on the surface of CNFs-PEI. These surface amine groups obstructed the hydrogen bonding formation during the freeze-drying process of CNFs-PEI, leading to less agglomerates in the film.

3.2. Characterization of the curing behaviors

The curing reactions between CNFs-PEI and epoxy were studied by DSC at four different heating rates (5, 10, 15, and 20 ^{o}C/min), and the typical DSC curves are shown in Figure 3. Compared with the flat DSC curve of the curing agent free epoxy system (Figure S4), the emerging exothermic peaks in the thermograms of CNFs-PEI/Epoxy manifested that the amine groups on CNFs-PEI could react with epoxy (Barton, 1985). The thermal analysis data associated with the curing reaction

(T_p, the peak temperature; ΔH, the enthalpy of the curing reaction) are summarized in Table 1. The peak temperature and the enthalpy of the curing reaction increased with the increase of heating rate. To have a better understanding of the curing process, the curing kinetics were studied using the Kissinger's method (Kissinger, 1957) and the Crane's method (Crane, Dynes, & Kaelble, 1973).

$$d\ln\left(\varphi / T_p^{\,2}\right) / d\left(1/Tp\right) = -\Delta E / R \tag{2}$$

$$d\ln\varphi / d(1/T_p) = -\left\lfloor \Delta E /(nR) + 2T_p \right\rfloor \tag{3}$$

where ΔE is the activation energy (kJ/mol) of curing, φ is the heating rate (°C/min), T_p is the maximum temperature (°C), n is the reaction order, and R is the ideal gas constant.

The plot of the Kissinger equations was shown in Figure 3b. The calculated activation energy for CNFs-PEI curing was 63.93 kJ/mol, higher than that for DDM curing (49.74 kJ/mol). The large volume of PEI molecule and the presence of CNFs might cause the steric effect, lowering the reactivity of the amine groups on PEI. The reaction order n calculated from the slope of Crane (Figure 3c) for the CNFs-PEI curing was 0.906, which was close to that for DDM (0.874). As references, the DSC curves of epoxy with DDM, and the corresponding Kissinger's plot and Crane's plot were shown in Figure S5.

To further reveal the curing ability of CNFs-PEI, the influence of CNFs-PEI content on the gel fraction of epoxy was investigated and the results are shown in Table 2. With the increase of CNFs-PEI content from 5% to 30%, the gel fraction increased from 12.65% to 60.19%. The results illustrated that the abundant amine groups on CNFs-PEI had effectively cured the epoxy. It is important to note that the amine groups were anchored at the CNFs' surface through covalent bonds. Therefore the curing density was not homogeneous in the composite. The curing density was high at the interphase between CNFs and epoxy, whereas other places of epoxy may not be cured. In order to cure the whole system, it is necessary to add a certain amount of additional DDM into the CNFs-PEI/Epoxy systems.

3.3. Characterization of the mechanical properties

The reinforcing effect of CNFs-PEI on nanocomposites was first evaluated by tensile testing, and the results are shown in Figure 4 and S6 (the representative stress-strain curves). The tensile strength and Young's modulus of neat epoxy film were 55.67 MPa and 1.01 GPa, respectively. For CNFs/Epoxy nanocomposites, the incorporation of CNFs made 33.83% and 201.98% increase in tensile strength (74.4 MPa) and Young's modulus (3.05 GPa), respectively. In comparison, for the CNFs-PEI/Epoxy nanocomposites, the increase was up to 88.11% in tensile strength (104.72MPa) and 237.63% in Young's modulus (3.41 GPa), respectively. DMA was also used to investigate the mechanical properties of the nanocomposites. Figure 4c and 4d depicted the tensile storage modulus (E') and the loss factor (Tan δ) of the nanocomposite films as a function of temperature, respectively. The neat epoxy displayed the typical behavior of an amorphous polymer material (Rahmanian, Suraya, Shazed, Zahari, & Zainudin, 2014). Among the three samples, the CNFs-PEI/Epoxy exhibited the highest storage modulus. The E' at 30 ^{o}C increased from 2.04 GPa for neat epoxy to 5.61 GPa for the CNFs-PEI/Epoxy nanocomposites. A more significant increase of E' was observed at the temperature above Tg. At 200^{o}C, for example, E' of the CNFs-PEI/Epoxy was 1338 MPa, representing 63-fold and 2.5-fold enhancement over that of the neat epoxy (21.2 MPa) and CNFs/Epoxy (531.1 MPa), respectively. These results consistently suggested that the reinforcement of CNFs-PEI was much better as compared with that of unmodified CNFs. In addition, the height of tan δ peaks substantially decreased for both nanocomposite films, and the peak for CNFs-PEI/Epoxy was the lowest, indicating that the energy dissipation process slowed down with the incorporation of nanofibers. It was interesting to note that the Tg of CNFs/Epoxy shifted toward a lower temperature (Figure 4d). Some researchers have reported similar results previously (Liao, Wu, Wu, Zhan, & Liu, 2012; Chen, Cao, & Feng, 2014). It could be attributed to several reasons. First, the CNFs were not dispersed homogenously in the matrix, and some part of the epoxy matrix was free of the reinforcing fibers (Liao, Wu, Wu, Zhan, & Liu, 2012). Second, the curing reaction between the hardener and the epoxy matrix might be hampered by the fillers, leading

to a reduced crosslinking density (Chen, Cao, & Feng, 2014). Nevertheless, compared with CNFs/Epoxy, CNFs-PEI/Epoxy exhibited a relatively higher Tg, which was very close to that of neat epoxy. It indicated that the better dispersion of CNFs-PEI and improved interfacial adhesion could compromise those adverse factors discussed above. As a result, the reinforcement of CNFs-PEI on epoxy was not only higher than that of cellulose fibers (Lu et al., 2013; Lu, Askeland, & Drzal, 2008), but also some carbon nanotubes (Rahmanian, Suraya, Shazed, Zahari, & Zainudin, 2014; Ayatollahi, Shadlou, Shokrieh, & Chitsazzadeh, 2011).

SEM images of the fractured surface of nanocomposites are shown in Figure 5. The neat epoxy has a rather smooth fractured surface, whereas a hierarchical surface morphology was observed for the CNFs/Epoxy. The clean surface of CNFs together with the large gaps between the CNFs bundles and the epoxy matrix (indicated by the arrows in Figure 5b) suggested that the interfacial adhesion was weak. By contrast, the dispersion of CNFs-PEI in epoxy was more uniform and the interface was blurred (Figure 5c). In addition, several CNFs-PEI which had been pulled out from the matrix were observed to have a thin epoxy coating (indicated by the red arrows in Figure 5c), suggesting that the interfacial adhesion was strengthened after PEI modification. The covalent bonds could allow efficient stress transfer from matrix to fibers, thereby enhancing the mechanical properties of the nanocomposites. Moreover, the surface of CNFs became much rougher after PEI grafting (Figure 2c), which may create a mechanical interlocking effect to prevent the pull out of CNFs.

3.4. Characterization of CTE and thermal conductivity

CTE is considered to be an important thermophysical parameter of polymer composites for engineering applications. For composite materials, the CTE is dependent on each component and their interfacial interactions (Wang et al., 2007). As shown in Table 3, the CTEs of both CNFs/Epoxy (38.17 ppm/K) and CNFs-PEI/Epoxy (22.19 ppm/K) were much lower than that of neat epoxy (88.60 ppm/K). The thermal expansion of the nanocomposites was remarkably impeded by

the incorporation of CNFs, due to the very low CTE value of cellulose (Yano, Sasaki, Shams, Abe, & Date, 2014). As expected, the CTE of CNFs-PEI/Epoxy was the lowest among the three samples, and a 74.95% reduction of CTE value was recorded for the CNFs-PEI/Epoxy. This was of great advantages for many applications such as the circuit board manufacturing where high thermal dimensional stability of the materials was a must (Wang et al., 2007).

In the meantime, when applied in electronic devices, a high thermal conductivity of epoxy is desired in order to prevent the material from overheating. As shown in Table 3, the thermal conductivity of CNFs-PEI/Epoxy (0.308 W/mK) was the highest, demonstrating a 35.01% enhancement over that of neat epoxy (0.228 W/mK). In contrast to the amorphous epoxy, the CNFs contain crystallized cellulose chains. The phonon scattering in the CNFs was weaker than that in epoxy (Shimazaki et al., 2007). The CNFs could produce tremendous pathways for phonon transfer in the nanocomposites, leading to the higher thermal conductivity of the nanocomposites.

4. Conclusion

In this work, PEI-grafted CNFs were synthesized as the reinforcing filler as well as the curing agent to prepare CNFs-PEI/Epoxy nanocomposites. The PEI functionalization increased the crosslinking density at the interphase between CNFs and Epoxy, leading to stronger interfacial interaction. Compared with neat epoxy, the mechanical properties of the nanocomposites were greatly improved. In addition, the incorporation of CNFs-PEI also remarkably reduced the CTE of the epoxy nanocomposites and improved their thermal conductivity, rendering the nanocomposites a board application in particular in electronic devices. To conclude, this study provided a valuable guidance for the rational design of high performance CNFs/Epoxy nanocomposites by tailoring the surface chemistry of CNFs.

Acknowledgements

The authors would like to thank National Natural Science Foundation of China

(51303112, 51473100 and 51433006), Excellent Young Scholar Fund of Sichuan University (2015SCU04A26) and State Key Laboratory of Polymer Materials Engineering (sklpme2016-3-09) for the financial support of this work.

Supplementary data

Supplementary data associated with this article can be found, in the online version.

References

Akil, H. M., Omar, M. F., Mazuki, A. A. M., Safiee, S., Ishak Z. A. M., & Bakar, A. A. (2011). Kenaf fiber reinforced composites: A review. *Materials & Design*, *32*, 4107-4121.

Ansari, F., Skrifvars M., & Berglund, L. (2015). Nanostructured biocomposites based on unsaturated polyester resin and a cellulose nanofiber network. *Composites Science and Technology*, *117*, 298-306.

Ashori, A., Babaee, M., Jonoobi M., & Hamzeh, Y. (2014). Solvent-free acetylation of cellulose nanofibers for improving compatibility and dispersion. *Carbohydrate Polymers*, *102*, 369-375.

Ayatollahi, M. R., Shadlou, S., Shokrieh M. M., & Chitsazzadeh, M. (2011). Effect of multi-walled carbon nanotube aspect ratio on mechanical and electrical properties of epoxy-based nanocomposites. *Polymer Testing*, *30*, 548-556.

Barton, J. M. (1985). The application of differential scanning calorimetry (DSC) to the study of epoxy resin curing reactions. *Epoxy resins and composites I*, *72*, 111-154.

Chen, S., Cao Y., & Feng, J. (2014). Polydopamine As an Efficient and Robust Platform to Functionalize Carbon Fiber for High-Performance Polymer Composites. *ACS Applied Materials & Interfaces*, *6*, 349-356.

Crane, L. W., Dynes P. J., & Kaelble, D. H. (1973). Analysis of curing kinetics in polymer composites. *Journal of Polymer Science Part B: Polymer Physics*, *11*, 533-540.

Inui, T., Koga, H., Nogi, M., Komoda N., & Suganuma, K. (2015). A miniaturized flexible antenna printed on a high dielectric constant nanopaper composite. *Advanced Materials*, *27*, 1112-1116.

Jia, X., Chen, G., Yu, Y., Li, G., Zhu, J., Luo, X., Duan, C., Yang X., & Hui, D. (2013). Effect of geometric factor, winding angle and pre-crack angle on quasi-static crushing behavior of filament wound CFRP cylinder. *Composites Part B: Engineering*, *45*, 1336-1343.

Kargarzadeh, H., Sheltami, R. M., Ahmad, I., Abdullah I., & Dufresne, A. (2015). Cellulose nanocrystal: A promising toughening agent for unsaturated polyester nanocomposite. *Polymer*, *56*, 346-357.

Kissinger, H. E. (1957). Reaction kinetics in differential thermal analysis. *Analytical Chemistry*, *29*, 1702-1706.

Klemm, D., Kramer, F., Moritz, S., Lindstrm, T., Ankerfors, M., Gray D., & Dorris, A. (2011). Nanocelluloses: A new family of nature-based materials. *Angewandte Chemie International Edition*, *50*, 5438-5466.

Liao, H., Wu, Y., Wu, M., Zhan X., & Liu, H. (2012). Aligned electrospun cellulose fibers reinforced epoxy resin composite films with high visible light transmittance. *Cellulose*, *19*, 111-119.

Liu B., & Huang, Y. (2011). Polyethyleneimine modified eggshell membrane as a novel biosorbent for adsorption and detoxification of Cr (VI) from water. *Journal of Materials Chemistry*, *21*, 17413-17418.

Liu, D., Pourrahimi, A. M., Olsson, R. T., Hedenqvist M. S., & Gedde, U. W. (2015). Influence of nanoparticle surface treatment on particle dispersion and interfacial adhesion in low-density polyethylene/aluminium oxide nanocomposites. *European Polymer Journal*, *66*, 67-77.

Low, I. M., McGrath, M., Lawrence, D., Schmidt, P., Lane, J., Latella, B. A., & Sim, K. S. (2007). Mechanical and fracture properties of cellulose-fibre-reinforced epoxy laminates. *Composites Part A: Applied Science and Manufacturing*, *38*, 963–974.

Lu, J., Askeland P., & Drzal, L. T. (2008). Surface modification of microfibrillated

cellulose for epoxy composite applications. *Polymer*, *49*, 1285-1296.

Lu, T., Jiang, M., Jiang, Z., Hui, D., Wang Z., & Zhou, Z. (2013). Effect of surface modification of bamboo cellulose fibers on mechanical properties of cellulose/epoxy composites. *Composites: Part B*, *51*, 28-34.

Lu, T., Liu, S., Jiang, M., Xu, X., Wang, Y., Wang, Z., Gou, J., Hui D., & Zhou, Z. (2014). Effects of modifications of bamboo cellulose fibers on the improved mechanical properties of cellulose reinforced poly (lactic acid) composites. *Composites: Part B*, *62*, 191-197.

Ma, L., Meng, L., Wu, G., Wang, Y., Zhao, M., Zhang C., & Huang, Y. (2015). Improving the interfacial properties of carbon fiber-reinforced epoxy composites by grafting of branched polyethyleneimine on carbon fiber surface in supercritical methanol. *Composites Science and Technology*, *114*, 64-71.

Masoodi, R., El-Hajjar, R. F., Pillai K. M., & Sabo, R. (2012). Mechanical characterization of cellulose nanofiber and bio-based epoxy composite. *Materials & Design*, *36*, 570-576.

Miao C., & Hamad, W. Y. (2013). Cellulose reinforced polymer composites and nanocomposites: a critical review. *Cellulose*, *20*, 2221-2262.

Missoum, K., Belgacem M. N., & Bras, J. (2013). Nanofibrillated Cellulose Surface Modification: A Review. *Materials*, *6*, 1745-1766.

Moon, R. J., Martini, A., Nairn, J., Simonsen J., & Youngblood, J. (2011). Cellulose nanomaterials review: structure, properties and nanocomposites. *Chemical Society Reviews*, *40*, 3941-3994.

Nishiyama, Y., Sugiyama, J., Chanzy H., & Langan, P. (2003). Crystal structure and hydrogen bonding system in cellulose Iα from synchrotron X-ray and neutron fiber diffraction. *Journal of the American Chemical Society*, *125*, 14300-4306.

Omrani, A., Simon L. C., & Rostami, A. A. (2008). Influences of cellulose nanofiber on the epoxy network formation. *Materials Science and Engineering: A*, *490*, 131-137.

Rahmanian, S., Suraya, A. R., Shazed, M. A., Zahari R., & Zainudin, E. S. (2014). Mechanical characterization of epoxy composite with multiscale reinforcements:

carbon nanotubes and short carbon fibers. *Materials & Design*, *60*, 34-40.

Sakakibara, K., Yano, H., & Tsujii Y., (2016). Surface Engineering of Cellulose Nanofiber by Adsorption of Diblock Copolymer Dispersant for Green Nanocomposite Materials. ACS Applied Materials & Interfaces, DOI: 10.1021/acsami.6b07769.

Shimazaki, Y., Miyazaki, Y., Takezawa, Y., Nogi, M., Abe, K., Ifuku S., & Yano, H. (2007). Excellent thermal conductivity of transparent cellulose nanofiber/epoxy resin nanocomposites. *Biomacromolecules*, *8*, 2976-2978.

Song M., & Xu, J. (2013). Preparation of Polyethylenimine‐Functionalized Graphene Oxide Composite and Its Application in Electrochemical Ammonia Sensors. *Electroanalysis*, *25*, 523-530.

Suzuki, K., Sato, A., Okumura, H., Hashimoto, T., Nakagaito, A. N., & Yano, H. (2014). Novel high-strength, micro fibrillated cellulose-reinforced polypropylene composites using a cationic polymer as compatibilizer. Cellulose, 21, 507–518.

Tang, X.-Z., Yu, B., Hansen, R. V., Chen, X., Hu X., & Yang, J. (2015). Grafting Low Contents of Branched Polyethylenimine onto Carbon Fibers to Effectively Improve Their Interfacial Shear Strength with an Epoxy Matrix. *Advanced Materials Interfaces*, *2*, 1500122-1500129.

Wang, S., Liang, Z., Gonnet, P., Liao, Y.-H., Wang B., & Zhang, C. (2007). Effect of nanotube functionalization on the coefficient of thermal expansion of nanocomposites. *Advanced Functional Materials*, *17*, 87-92.

Xie, Y., Hill, C. A. S., Xiao, Z., Militz H., & Mai, C. (2010). Silane coupling agents used for natural fiber/polymer composites: A review. *Composites: Part A*, *41*, 806-819.

Yang, X., Shi, K., Zhitomirsky, I., & Cranston, E. D. (2015). Cellulose Nanocrystal Aerogels as Universal 3D Lightweight Substrates for Supercapacitor Materials. *Advanced Materials*, *27*, 6104-6109.

Yano, H., Sasaki, S., Shams, M. I., Abe K., & Date, T. (2014). Wood Pulp-Based Optically Transparent Film: A Paradigm from Nanofibers to Nanostructured Fibers. *Advanced Optical Materials*, *2*, 231-234.

Zhang, Q., Wang, N., Xu T., & Cheng, Y. (2012). Poly(amidoamine) dendronized hollow fiber membranes: Synthesis, characterization, and preliminary applications as drug delivery devices. *Acta Biomaterialia*, *8*, 1316-1322

Zhang, W., Zhang, Y., Lu C., & Deng, Y. (2012). Aerogels from crosslinked cellulose nano/micro-fibrils and their fast shape recovery property in water. *Journal of Materials Chemistry*, *22*, 11642-11650.

Zhao, J., Lu, C., He, X., Zhang, X., Zhang W., & Zhang, X. (2015). Polyethylenimine-Grafted Cellulose Nanofibril Aerogels as Versatile Vehicles for Drug Delivery. *ACS Applied Materials & Interfaces*, *7*, 2607-2615.

Zhou, W. (2011). Effect of coupling agents on the thermal conductivity of aluminum particle/epoxy resin composites. *Journal of Materials Science*, *46*, 3883-3889.

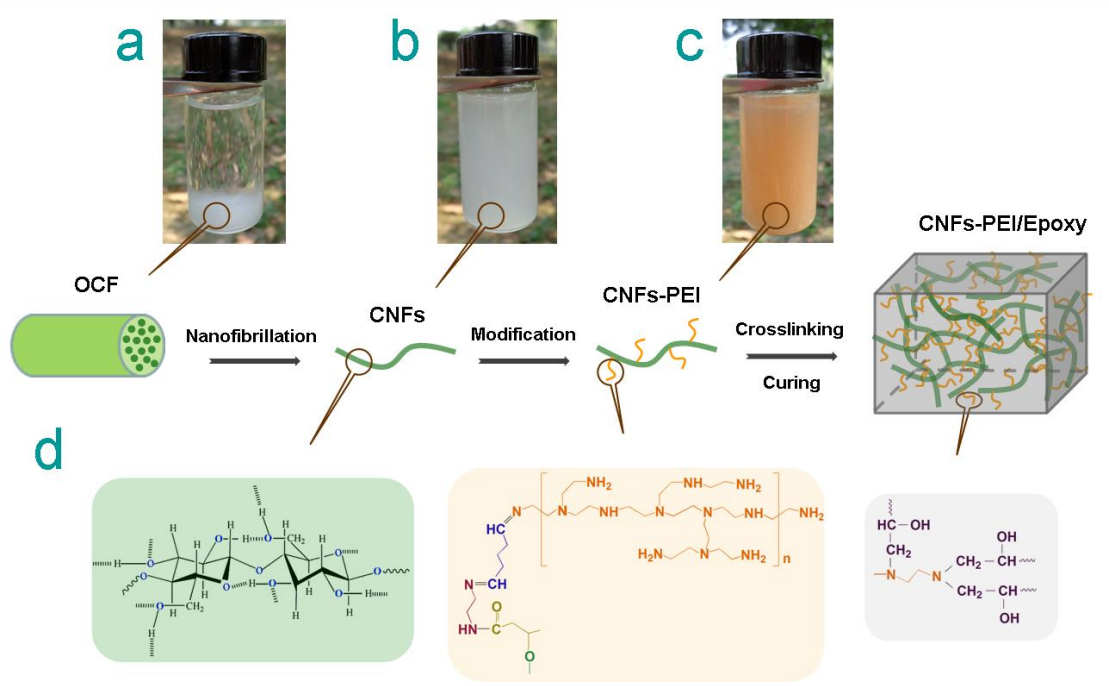

Figure 1. Photographs of the water dispersions of (a) OCF, (b) CNFs and (c) CNFs-PEI after three days standing. (d) The schematic of the synthesis of CNFs-PEI/Epoxy nanocomposites.

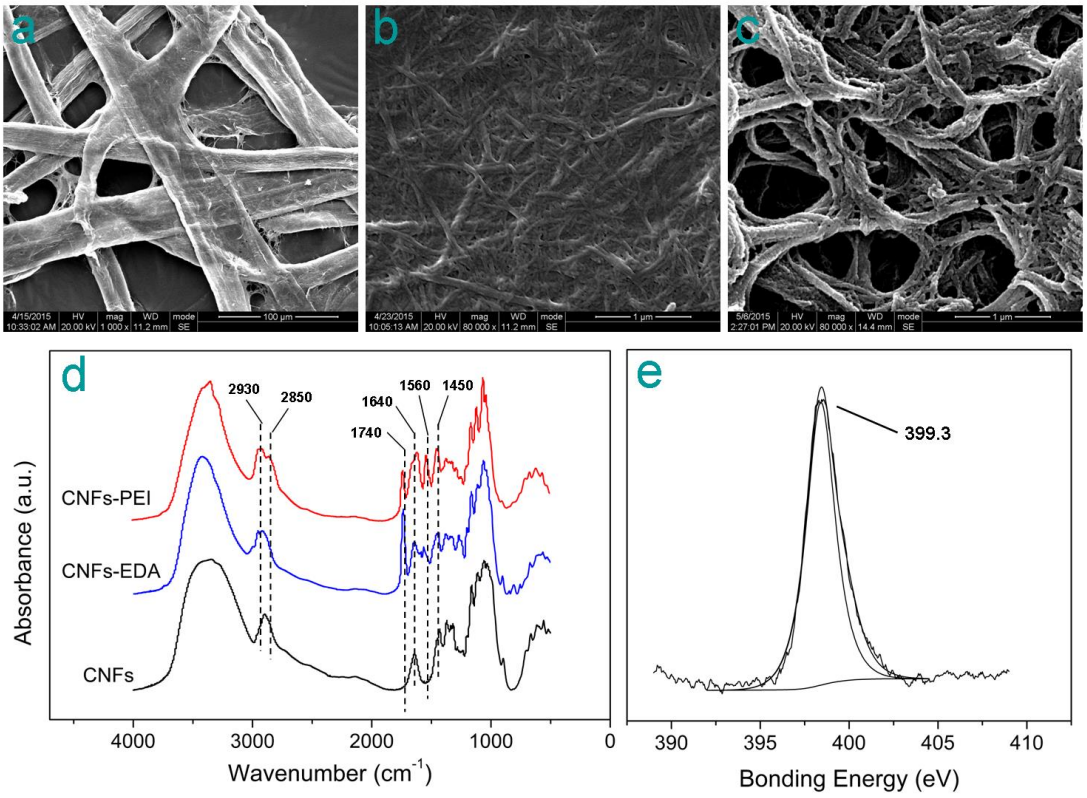

Figure 2. SEM images of the (a) OCFs, (b) CNFs and (c) CNFs-PEI. (d) FTIR spectra for CNFs, CNFs-EDA, and CNFs-PEI. (e) XPS N1s core-level spectra of CNFs-PEI.

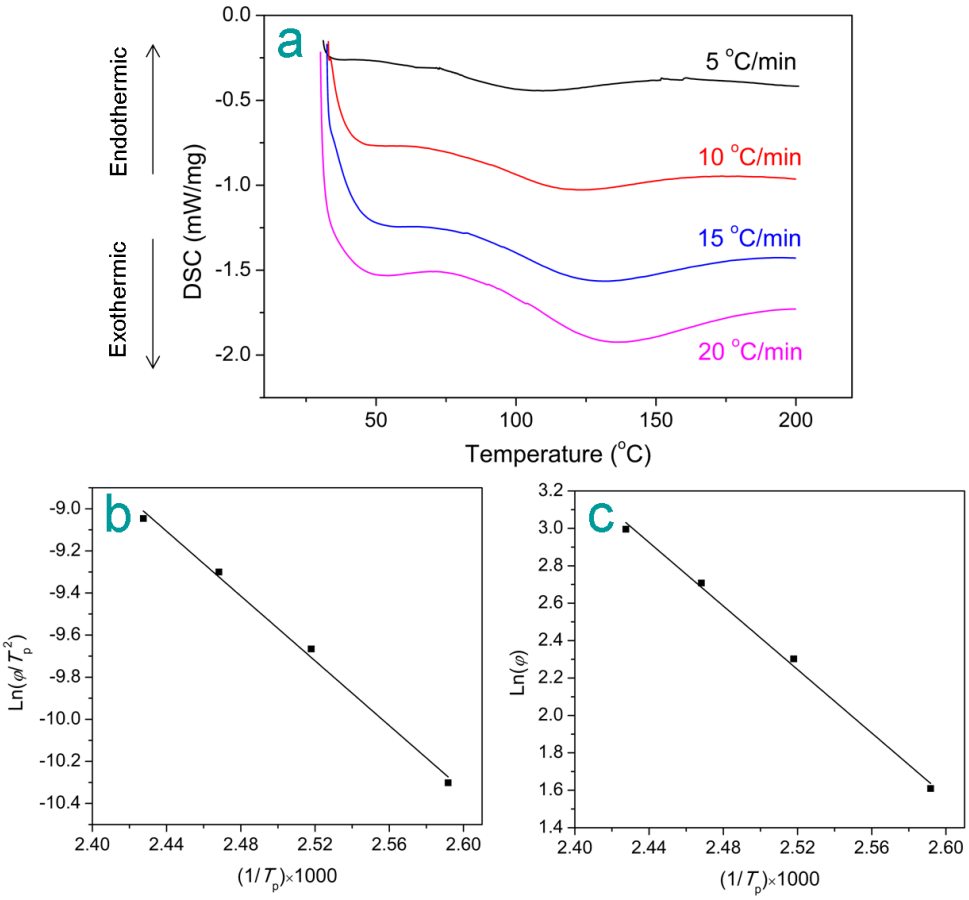

Figure 3. (a) The typical DSC curves of CNFs-PEI/Epoxy blend at different heating rates. (b) Kissinger's plot of $\ln(\varphi/T_p^2)$ versus $1/T_p$. (c) Crane's plot of $\ln(\varphi)$ versus $1/T_p$.

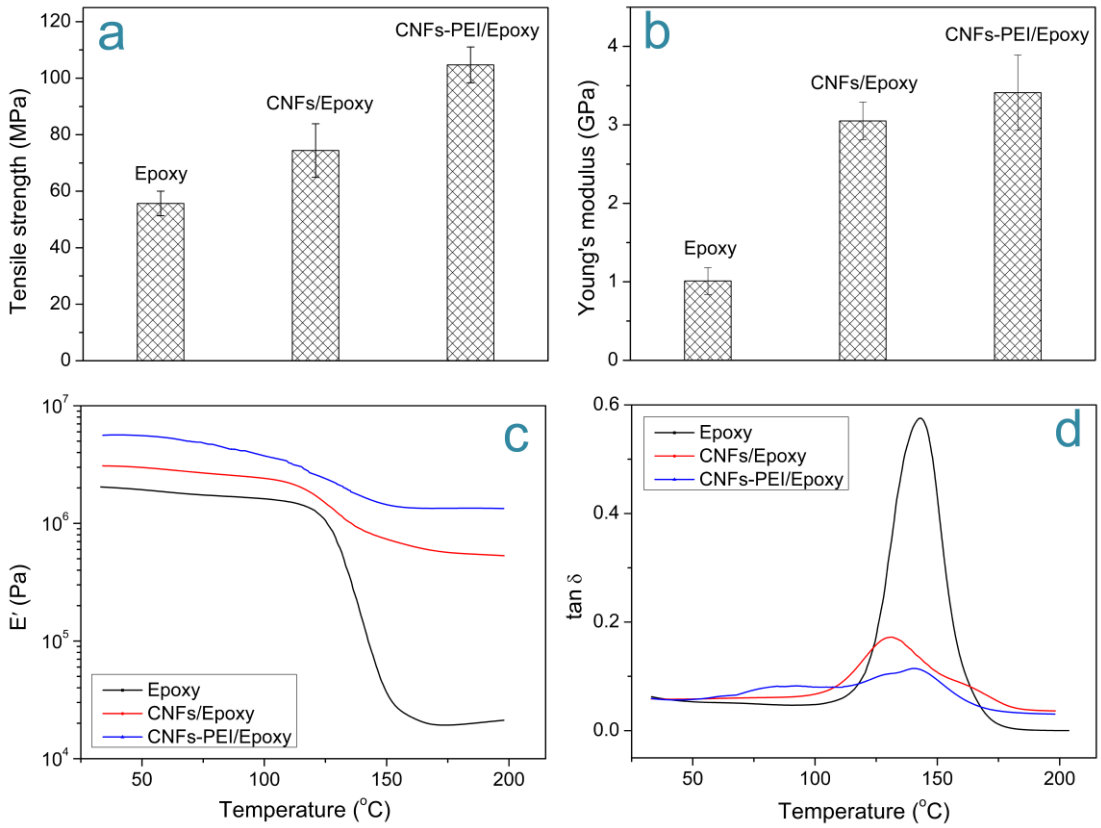

Figure 4. (a) Tensile strength and (b) Young modulus of the nanocomposites. (c) Storage modulus (E) and (d) loss factor (Tan δ) *vs* temperature curves of the nanocomposites.

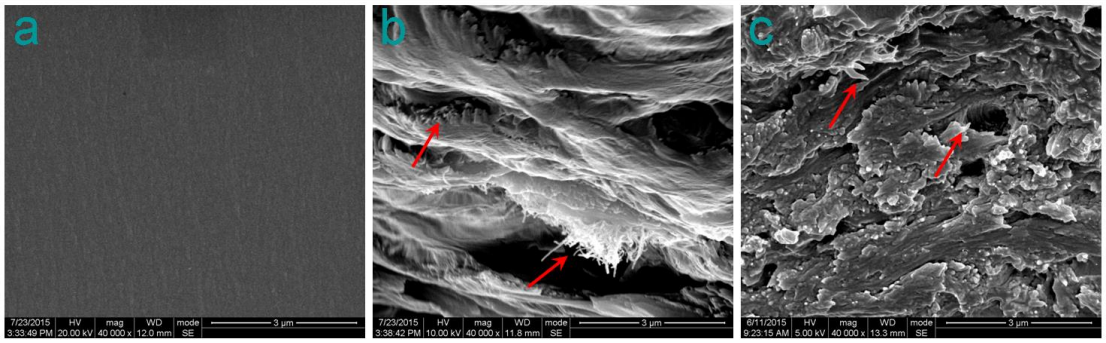

Figure 5. SEM images of the fractured surfaces for (a) neat epoxy, (b) CNFs/Epoxy and (c) CNFs-PEI/Epoxy.

Table 1. Curing reaction data from DSC at different heating rate.

φ (^{o}C/min)	Tp (^{o}C)	ΔE (kJ/mol)
5	112.7	13.0
10	124.0	18.2
15	132.0	28.1
20	138.8	36.6

Table 2. The effect of CNFs-PEI content on the gel fraction of epoxy.

CNFs-PEI content (%)	Gel fraction (%)
5	12.65
10	22.14
20	40.88
30	60.19

Table 3. The CTE and thermal conductivity data of the nanocomposite films

Sample	CTE (ppm/K)	thermal conductivity (W/mK)
Epoxy	88.60	0.228
CNFs/Epoxy	38.17	0.269
CNFs-PEI/Epoxy	22.19	0.308